The Astronomical Journal, 151:37 (8pp), 2016 February doi:10.3847/0004-6256/151/2/37

SOUTH GALACTIC CAP *u*-BAND SKY SURVEY (SCUSS): DATA RELEASE

Hu Zou[1], Xu Zhou[1], Zhaoji Jiang[1], Xiyan Peng[1], Dongwei Fan[1], Xiaohui Fan[2], Zhou Fan[1], Boliang He[1], Yipeng Jing[3], Michael Lesser[2], Cheng Li[4], Jun Ma[1], Jundan Nie[1], Shiyin Shen[4], Jiali Wang[1], Zhenyu Wu[1], Tianmeng Zhang[1], and Zhimin Zhou[1]

[1] Key Laboratory of Optical Astronomy, National Astronomical Observatories, Chinese Academy of Sciences, Beijing, 100012, China; zouhu@nao.cas.cn

[2] Steward Observatory, University of Arizona, Tucson, AZ 85721, USA

[3] Center for Astronomy and Astrophysics, Department of Physics and Astronomy, Shanghai Jiao Tong University, Shanghai 200240, China

[4] Shanghai Astronomical Observatory, Chinese Academy of Sciences, Shanghai 200030, China

Received 2015 November 1; accepted 2015 December 23; published 2016 January 28

ABSTRACT

The South Galactic Cap *u*-band Sky Survey (SCUSS) is a deep *u*-band imaging survey in the south Galactic cap using the 2.3 m Bok telescope. The survey observations were completed at the end of 2013, covering an area of about 5000 square degrees. We release the data in the region with an area of about 4000 deg^2 that is mostly covered by the Sloan digital sky survey. The data products contain calibrated single-epoch images, stacked images, photometric catalogs, and a catalog of star proper motions derived by Peng et al. The median seeing and magnitude limit (5σ) are about 2$''$.0 and 23.2 mag, respectively. There are about 8 million objects having measurements of absolute proper motions. All the data and related documentations can be accessed through the SCUSS data release website http://batc.bao.ac.cn/Uband/data.html.

Key words: catalogs – surveys – techniques: image processing – techniques: photometric

1. INTRODUCTION

The South Galactic Cap *u*-band Sky Survey (SCUSS) is an international cooperative project between the National Astronomical Observatories of Chinese Academy of Sciences and the Steward Observatory of the University of Arizona (X. Zhou et al. 2015, in preparation). The survey was originally planned to perform a sky survey of about 3700 deg^2 in the south Galactic cap by using the 2.3 m Bok telescope. The project was initiated in fall 2009 and its first run started in 2010 September. The survey ended its observation in 2013 December. The final survey area is about 5000 deg^2, far beyond the planned area.

The main goal of the survey is to supply a *u*-band catalog for the spectroscopic target selection of the Large Sky Area Multi-Object Fiber Spectroscopy Telescope (Cui et al. 2012). Besides, combined with the *g*, *r*, *i*, and *z*-band data of the Sloan Digital Sky Survey (SDSS; York et al. 2000), the deep SCUSS *u*-band data can be used to study the Milk Way and galaxies. A series of papers based on the SCUSS data have been published, including investigating the halo structure of the Galaxy (Nie et al. 2015), calculating star proper motions (Peng et al. 2015), estimating the Galactic photometric metallicity and model parameters (Jia et al. 2014; Gu et al. 2015), and selecting spectroscopic targets, such as quasars and emission line galaxies (Comparat et al. 2015; Raichoor et al. 2015; Zou et al. 2015b).

This paper describes the data set of the SCUSS data release that is made publicly available. The paper is organized as follows: Section 2 summarizes the survey and data reduction; Section 3 presents the data products including the calibrated images and photometric catalogs; Section 4 gives an analysis of the data quality; Section 5 describes the catalog of star proper motions derived by Peng et al. (2015); and Section 6 is the conclusion.

2. THE SURVEY AND DATA REDUCTION

The SCUSS is a wide and deep *u*-band sky survey in the south Galactic cap. The survey uses the 90 inch (2.3 m) Bok telescope that belongs to the Steward Observatory. It operates every night of the year except Christmas Eve and the maintenance period in August. The camera, named 90Prime, is installed at the prime focus (correct focal ratio $f/2.98$). It contains four 4k × 4k backside-illuminated CCDs that are assembled in a 2 × 2 array with gaps along both vertical and horizontal directions. The CCDs are optimized for the *u*-band response, giving a quantum efficiency close to 80%. The edge-to-edge FOV is about 1°.08 × 1°.03. The adopted filter is similar to the SDSS *u* band. The SCUSS *u* filter is somewhat bluer and narrower. The central wavelength and FWHM are 3538 and 520 Å, respectively (Zou et al. 2015a).

The originally designed survey footprint is located within the region of $\delta > -10^\circ$ and Galactic latitude $b < -30^\circ$. The observation started in 2010 September and ended in 2013 December. The final area is about 5000 deg^2 (dashed green line in Figure 1), including the planned area, an extra area in the northwest corner, and the region extending to the anti-Galactic center. In this paper, we only release the data shown in the blue area of Figure 1. The area is about 4000 deg^2, 92% of which is covered by the SDSS. Each field has two continuous exposures, giving a total exposure time of 5 minutes. These two exposures are dithered by 1/2 of the CCD size, which benefits the internal photometric calibration and gap filling. In this way, most of the field is covered by two exposures. Some gap areas are covered by one exposure. The exposure time of 5 minutes generates an expected depth of 23.0 mag.

The following is a summary of the data reduction. More details can be found in Zou et al. (2015a).

(1) Detrending: a dedicated image processing pipeline was compiled, which performs some standard calibrations (overscan subtraction, bias correction, and flat-fielding, etc.) and special handling (crosstalk, CCD artefacts, abnormal overscan, and sky gradient etc.)
(2) Astrometry: the UCAC4 catalogs are used to derive the astrometric solutions. The global external position error is

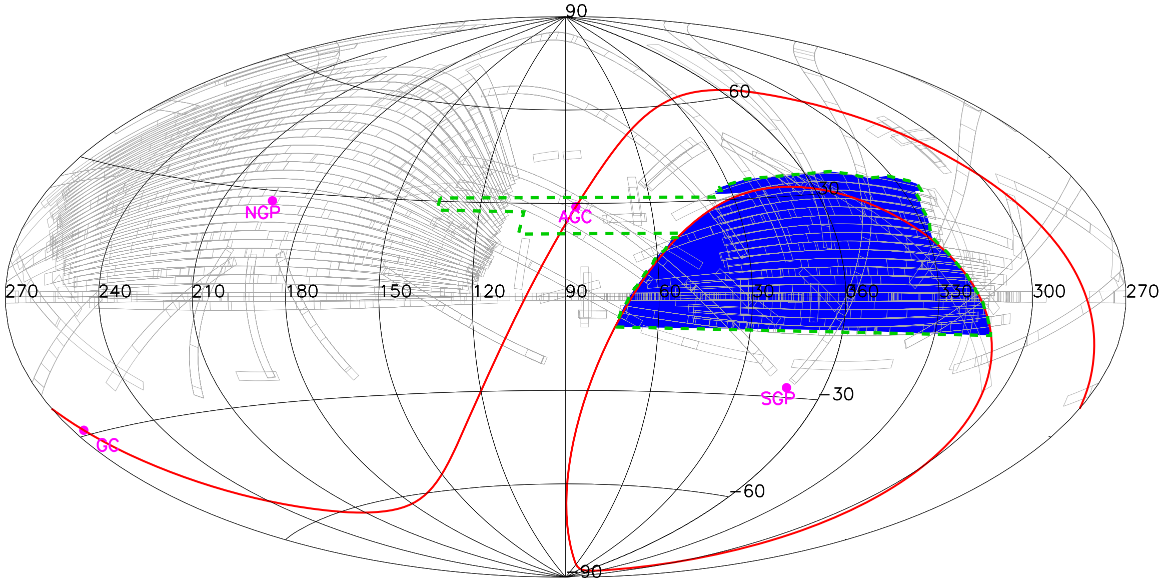

Figure 1. Aitoff projection of the SCUSS footprint. This projection is centered at ($\alpha = 90°$, $\delta = 0°$). Pink filled circles show the south Galactic pole (SGP), north Galactic pole (NGP), Galactic center (GC), and anti-Galactic center (AGC). The red solid curves show the Galactic plane and Galactic latitude of $-30°$. The green dashed lines present the actual coverage of the survey, whose area is about 5000 deg^2. The blue filled region is the area where the data are to be released in this paper. The SDSS imaging runs are also overlapped in gray.

Table 1
Main Keywords in the FITS Header of Single-epoch Images and Their Meanings

Keyword	Data Type	Meaning
RA-OBS	string	R.A. of the field center in J2000
DEC-OBS	string	Decl. of the field center in J2000
CCD_NO	int	CCD number
DATE-OBS	string	UTC date when the shutter was opened
TIME-OBS	string	UTC time when the exposure was started
EXPTIME	float	Exposure time (seconds)
RA	string	Right ascension in the specified epoch
DEC	string	Decl. in the specified epoch
HA	string	Hour angle
EPOCH	float	Equinox for R.A. and Decl.
FILTER	string	Filter name
OBJECT	string	Field name
RDNOCAL	string	Calculated readout noises for four CCDs
GAINCAL	string	Calculated gains for four CCDs
SKYADU	float	Sky background in DN
SEEING	float	Seeing in arcsec
A81	double	Coefficients for coordinate transformation
A82	double	Coefficients for coordinate transformation
A83	double	Coefficients for coordinate transformation
A84	double	Coefficients for coordinate transformation
A85	double	Coefficients for coordinate transformation
A86	double	Coefficients for coordinate transformation
A87	double	Coefficients for coordinate transformation
A88	double	Coefficients for coordinate transformation
AIRMASS	float	Airmass when the exposure was taken
MAZIMUTH	float	Moon azimuth in degrees from south through west
MALITIUD	float	Moon altitude in degrees
MANGLE	float	Position angle of moon relative to the camera center
CALIA73	float	Zeropoint for the whole CCD image
CALIA731	float	Zeropoint for the Amp. #1. of the CCD image
CALIA732	float	Zeropoint for the Amp. #2. of the CCD image
CALIA733	float	Zeropoint for the Amp. #3. of the CCD image
CALIA734	float	Zeropoint for the Amp. #4. of the CCD image

about 0.″13. The average internal astrometric error, from sources on overlapping exposures, is about 0.″09.

(3) Magnitude calibrations: the SDSS catalogs are used to make external photometric calibrations. We calculate the photometric zeropoints (ZPs) separately for the four amplifiers to reduce the effect of gain and photometric response variations. For images out of the SDSS coverage, we interactively derive their photometric ZPs internally by using the common stars in the overlapped area.

(4) Image stacking: single-epoch images with specified qualities are stacked. More than 91% of stacked images are assembled by using single-epoch images with consistent qualities.

(5) Photometry: SExtractor photometry (Bertin & Arnouts 1996) with automatic elliptical apertures is performed on stacked images. The aperture, point-spread function (PSF), and model magnitudes are measured from both stacked images and co-added flux measurements on single-epoch images. The model photometry uses the SDSS r-band shape parameters. Due to improper flat-fielding, scattered light, and focal plane distortion, the photometric ZP would vary with the position in the CCD plane so that there are photometric residuals across the CCD. We derive such residual maps for all CCDs and use them to correct the magnitudes.

3. DATA PRODUCTS

3.1. Calibrated Images

Single-epoch images are calibrated by the dedicated image processing pipeline. There are a total of 44,937 images. The coordinate system adopts the ARC celestial projection, mostly used in Schmidt plate astrometry, with a second-order radial distortion. The coordinate transformation between the focal plane and the celestial coordinates can be made by using our

Table 2
Main Columns in SCUSS Photometric Catalogs

Field	Data type	Meaning
NUMBER	LONG	ID of objects in stacked images
RA2000	STRING	R.A. in J2000
DEC2000	STRING	Decl. in J2000
X	FLOAT	Image X of SDSS objects
Y	FLOAT	Image Y of SDSS objects
BER_X	FLOAT	SExtractor X of objects detected on stacked images
BER_Y	FLOAT	SExtractor Y of objects detected on stacked images
MAG_AUTO	FLOAT	Automatic magnitude derived by SExtractor
MAGERR_AUTO	FLOAT	Automatic magnitude error derived by SExtractor
KRON_RADIUS	FLOAT	Kron radius in pixels derived by SExtractor
MAG_PETRO	FLOAT	Petrosian magnitude derived by SExtractor
MAGERR_PETRO	FLOAT	Petrosian magnitude error derived by SExtractor
PETRO_RADIUS	FLOAT	Petrosian radius in pixels derived by SExtractor
FLUX_RADIUS	FLOAT	Half-light radius in pixels derived by SExtractor
FWHM_IMAGE	FLOAT	FWHM of objects in pixels derived by SExtractor
BERTIN_G_S	FLOAT	Stellarity (0 galaxy; 1 star) derived by SExtractor
A_AXIS	FLOAT	Length of the major axis in pixels derived by SExtractor
ELLIPTICITY	FLOAT	Ellipticity derived by SExtractor
THETA	FLOAT	Position angle in degrees derived by SExtractor
BERTIN_CLASS	INT	SExtractor Flags
COMBINE_NUMB	INT	Exposure number in the stacked image
PSFMAG	FLOAT	PSF magnitudes on the stacked image
PSFERR	FLOAT	PSF magnitude error on the stacked image
PSFFLAG	INT	Flags of the PSF magnitude on the stacked image
APMAG	DOUBLE	Aperture magnitude on the stacked image (12 apertures)
APMAGERR	DOUBLE	Aperture magnitude error on the stacked image
MODELMAG	FLOAT	Model magnitude on the stacked image
MODELMAGERR	FLOAT	Model magnitude error on the stacked image
PSFADD	DOUBLE	Co-added PSF magnitude from single-epoch images
PSFADDERR	DOUBLE	Co-added PSF magnitude error from single-epoch image
PSFADDSTD	DOUBLE	Standard deviation of the co-added PSF magnitude
PSFADDFLAG	LONG	Flags of the co-added PSF magnitude
PSFADDNUM	INT	Exposure number for the co-added PSF magnitude
APADD	DOUBLE	Co-added aperture magnitudes (12 apertures)
APADDERR	DOUBLE	Co-added aperture magnitude errors
APADDSTD	DOUBLE	Standard deviations of the co-added aperture magnitudes
APADDNUM	LONG	Exposure numbers for the co-added aperture magnitudes
MODELADD	FLOAT	Co-added model magnitude
MODELADDERR	FLOAT	Co-added model magnitude error.
MODELADDSTD	FLOAT	Standard deviation of the co-added model magnitude
MODELADDNUM	INT	Exposure number for the co-added model magnitude
JDMEAN	DOUBLE	Average Julian day for each object
MATCH_ERR	FLOAT	Match error in arcsec between SCUSS detected objects and SDSS objects

IDL/Python programs[5] with the eight coefficients in the FITS header (keywords of A81, A82, ..., and A88) and a second-order coefficient, which is implemented as inline functions in the programs. The usages of these programs can be found in the webpage.[6] The WCS parameters in the header are incorrect. The photometric ZPs of four amplifiers are presented in the keywords CALIA731, CALIA732, CALIA733, and CALIA734, which correspond to the northeast, southeast, northwest, and southwest quadrants of the image. Thus, the magnitude can be calculated as $m = -2.5\log_{10}F + 25 + \mathrm{ZP}$, where F is the measured flux in DN. To ensure homogeneity of the imaging depth and coverage completeness of the stacked images, we flag single-epoch images according to their qualities. The images with seeing $<3\farcs0$, sky ADU < 500, and ZP > 3.5 are flagged with "1." If a sky region does not have enough images flagged with "1," the corresponding images in this region with seeing $<3\farcs0$ are flagged with "2." If the region still does not have enough images to meet the depth requirement, the rest of the images located in this region are flagged with "3." For the remaining images, we flag the ones with seeing $<3\farcs0$ with "4" or otherwise with "5." Table 1 presents the main keywords in the FITS header of single-epoch images.

There are a total of 3700 stacked images, each of which has an area of $1\fdg08 \times 1\fdg04$ and about $1'$ overlaps with adjacent images. These stacked images are assembled with the single-epoch images flagged as "1," "2," and "3." The coordinate system is a purely linear transformation in the ARC celestial projection. The ZP is stored in the keyword CALIA73. The other header keywords are similar to those in the single-epoch images, but the WCS parameters are accurate enough. In

5 http://batc.bao.ac.cn/BASS/lib/exe/fetch.php?media=scuss:single-epoch_image_calibration:a8_convert.tar.gz
6 http://batc.bao.ac.cn/BASS/doku.php?id=scuss:single-epoch_image_calibration:idl_python_programs

Table 3
Main SDSS Columns Included in SCUSS Photometric Catalogs

Field	Data type	Meaning
SDSSOBJID	STRING	SDSS OBJID in SDSS DR9
SDSSTYPE	STRING	SDSS object type (s: star; g: galaxy)
PSFMAG_U	FLOAT	SDSS u-band PSF magnitude
PSFMAG_G	FLOAT	SDSS g-band PSF magnitude
PSFMAG_R	FLOAT	SDSS r-band PSF magnitude
PSFMAG_I	FLOAT	SDSS i-band PSF magnitude
PSFMAG_Z	FLOAT	SDSS z-band PSF magnitude
PSFMAGERR_U	FLOAT	SDSS u-band PSF magnitude error
PSFMAGERR_G	FLOAT	SDSS g-band PSF magnitude error
PSFMAGERR_R	FLOAT	SDSS r-band PSF magnitude error
PSFMAGERR_I	FLOAT	SDSS i-band PSF magnitude error
PSFMAGERR_Z	FLOAT	SDSS z-band PSF magnitude error
PETROMAG_U	FLOAT	SDSS u-band Petrosian magnitude
PETROMAG_G	FLOAT	SDSS g-band Petrosian magnitude
PETROMAG_R	FLOAT	SDSS r-band Petrosian magnitude
PETROMAG_I	FLOAT	SDSS i-band Petrosian magnitude
PETROMAG_Z	FLOAT	SDSS z-band Petrosian magnitude
PETROMAGERR_U	FLOAT	SDSS u-band Petrosian magnitude error
PETROMAGERR_G	FLOAT	SDSS g-band Petrosian magnitude error
PETROMAGERR_R	FLOAT	SDSS r-band Petrosian magnitude error
PETROMAGERR_I	FLOAT	SDSS i-band Petrosian magnitude error
PETROMAGERR_Z	FLOAT	SDSS z-band Petrosian magnitude error
MODELMAG_U	FLOAT	SDSS u-band model magnitude
MODELMAG_G	FLOAT	SDSS g-band model magnitude
MODELMAG_R	FLOAT	SDSS r-band model magnitude
MODELMAG_I	FLOAT	SDSS i-band model magnitude
MODELMAG_Z	FLOAT	SDSS z-band model magnitude
MODELMAGERR_U	FLOAT	SDSS u-band model magnitude error
MODELMAGERR_G	FLOAT	SDSS g-band model magnitude error
MODELMAGERR_R	FLOAT	SDSS r-band model magnitude error
MODELMAGERR_I	FLOAT	SDSS i-band model magnitude error
MODELMAGERR_Z	FLOAT	SDSS z-band model magnitude error
CMODELMAG_U	FLOAT	SDSS u-band Cmodel magnitude
CMODELMAG_G	FLOAT	SDSS g-band Cmodel magnitude
CMODELMAG_R	FLOAT	SDSS r-band Cmodel magnitude
CMODELMAG_I	FLOAT	SDSS i-band Cmodel magnitude
CMODELMAG_Z	FLOAT	SDSS z-band Cmodel magnitude
CMODELMAGERR_U	FLOAT	SDSS u-band Cmodel magnitude error
CMODELMAGERR_G	FLOAT	SDSS g-band Cmodel magnitude error
CMODELMAGERR_R	FLOAT	SDSS r-band Cmodel magnitude error
CMODELMAGERR_I	FLOAT	SDSS i-band Cmodel magnitude error
CMODELMAGERR_Z	FLOAT	SDSS z-band Cmodel magnitude error
EXTINCTION_U	FLOAT	SDSS u-band extinction
EXTINCTION_G	FLOAT	SDSS g-band extinction
EXTINCTION_R	FLOAT	SDSS r-band extinction
EXTINCTION_I	FLOAT	SDSS i-band extinction
EXTINCTION_Z	FLOAT	SDSS z-band extinction

addition, there is a weight map corresponding to each stacked image, giving the number of exposures.

3.2. Photometric Catalogs

The catalogs contain both magnitudes measured on stacked images and co-added magnitudes from measurements on single-epoch images. The objects come from the SCUSS detections and SDSS catalogs with any of the *ugriz* magnitudes in DR9 brighter than 23.5 mag. The matching error between the SCUSS and SDSS is 2″.0. In the catalogs, SDSS objects can be recognized by the NUMBER column, where NUMBER < 49,000 or 50,000 < NUMBER < 60,000. The SCUSS unique objects have NUMBER > 60,000. Extra matched fainter SDSS objects within 2″ have 49,000 < NUMBER < 50,000.

The SExtractor photometry is performed only on stacked images, providing the automatic magnitude, Kron radius, shape parameters, object classification, etc. Aperture, PSF, model magnitudes are measured on both stacked images and single-epoch images. Co-added magnitudes are derived from these measurements on single-epoch images. Flags for the PSF magnitude (column PSFFLAG) are coded in decimal and expressed as a sum of powers of 2: 1 for CCD artefacts; 2 for bad pixels; 4 for saturated pixels; 8 for contamination from neighbors; and 16 for edges of the image. The co-added flag (PSFADDFLAG) is the combination of corresponding flags of the same object measured on multiple single-epoch images.

If stack images are combined with single images of similar qualities, the magnitudes measured on stacked images are better than the co-added ones, since the object number is 20% higher. Conversely, the co-added magnitudes should be better. We can refer to Zou et al. (2015a) for the general guidelines to use the magnitudes. Tables 2 and 3 show both the SCUSS and SDSS photometric information included in the catalogs. All magnitudes are corrected to the aperture magnitudes (7″.26 in radius), which is also used for photometric calibrations.

4. DATA QUALITY AND DEPTH

The color–color diagram is an excellent tool to compare the photometry of the SCUSS and SDSS. Figure 2 shows the scatters of stars in the $u - g$ versus $g - r$ plane. These stars are spectroscopically identified by the SDSS. The SCUSS co-added PSF magnitude and SDSS PSF magnitudes are used for comparison. In this figure, the star sequence using the SCUSS u band is tighter. We select two color intervals of $1.3 < g - r < 1.6$ (mostly M-type stars) and $0.0 < g - r < 0.3$ (mostly A-type stars) to show the $u - g$ distributions, which is presented in Figure 3. The dispersion of the $u_{\rm SCUSS} - g$ color is smaller than that of the $u_{\rm SDSS} - g$. Moreover, objects located in the lower right (enclosed by a polygon in Figure 2) are identified as stars but initially selected as quasar candidates with redshift larger than 3.0. These stars were faint and mistakenly selected as quasars due to the bad SDSS u-band photometry. But they are still located in the star sequence when the SCUSS u band is used.

The SCUSS and SDSS u-band photometry is also compared by using the catalogs from the Canada–France–Hawaii Telescope Legacy Survey (CFHTLS), whose wide-field u-band depth reaches about 25.2 mag (80% completeness limit). We select the CFHTLS W4 field ($\alpha = 22^{\rm h}13^{\rm m}18^{\rm s}$, $\delta = +01^{\rm d}19^{\rm m}00^{\rm s}$) that is fully covered by the SCUSS. Figure 4 shows the photometric comparison of point sources that are classified by the SDSS. The SCUSS and SDSS u-band

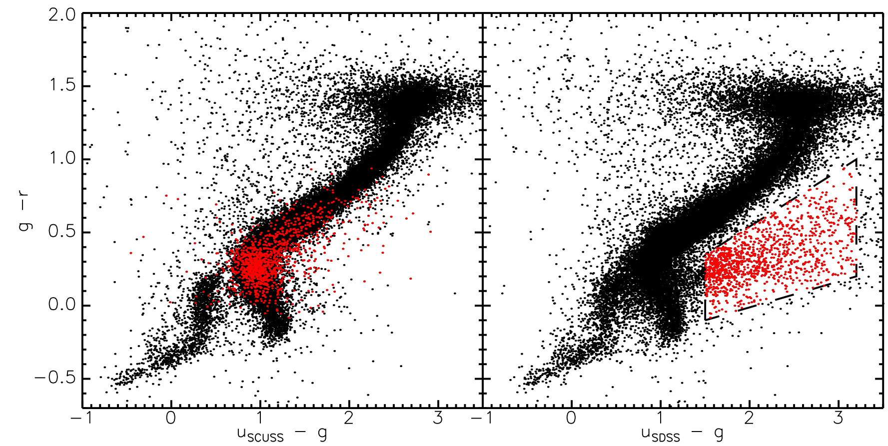

Figure 2. Left: stars spectroscopically identified by the SDSS in the color–color diagram of $u_{\rm SCUSS} - g$ vs. $g - r$. Right: the same stars in the color–color diagram of $u_{\rm SDSS} - g$ vs. $g - r$. The magnitudes are corrected for the Galactic extinction (Schlegel et al. 1998) and the color term used by Zou et al. (2015b). The dashed polygon indicates that the objects were initially selected as quasar candidates but identified by the SDSS as stars. Both the g- and r-band magnitudes come from the SDSS.

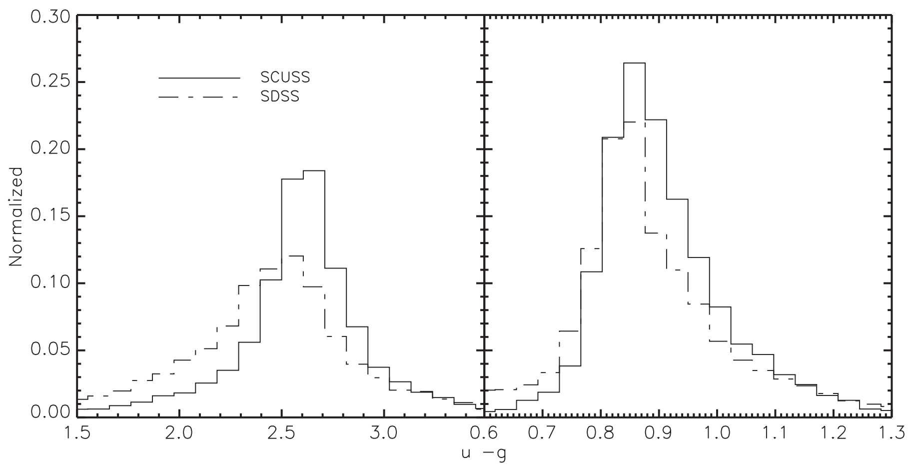

Figure 3. Left: the $u - g$ distribution of stars with $1.3 < g - r < 1.6$. Right: the $u - g$ distributions of stars with $0.0 < g - r < 0.3$. The solid and dashed histograms use the SCUSS and SDSS u bands, respectively.

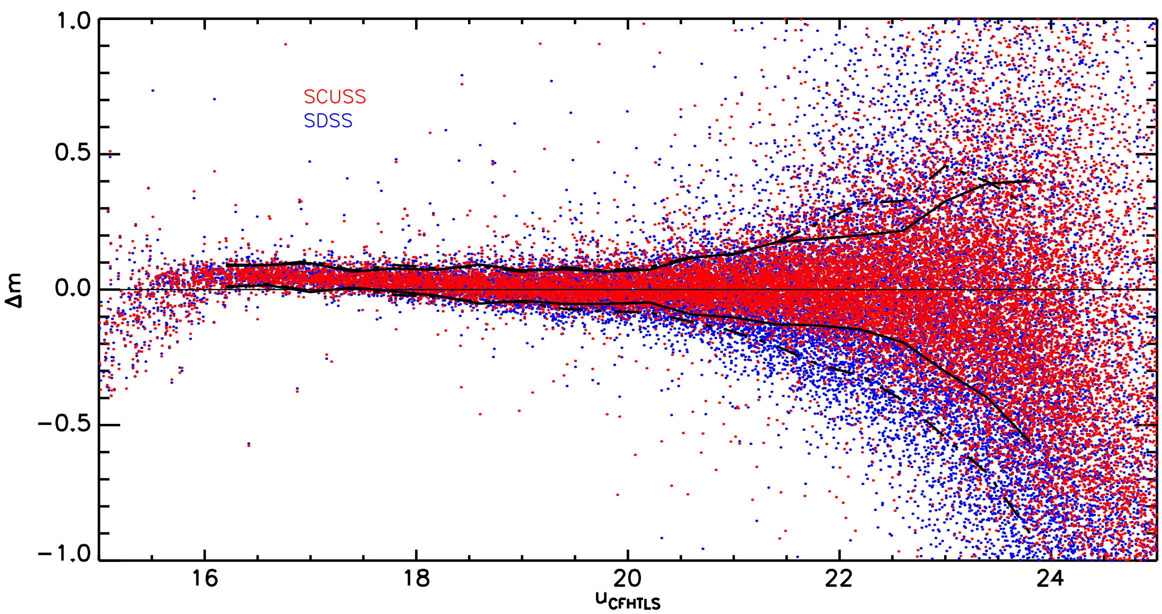

Figure 4. The u-band magnitude difference between the SCUSS/SDSS and the CFHTLS as a function of the CFHTLS u-band magnitude. The blue points stand for the SDSS and the red ones stand for the SCUSS. The solid and dashed lines show the rms around the average as a function of the CHFTLS u-band magnitude for the SCUSS and SDSS, respectively.

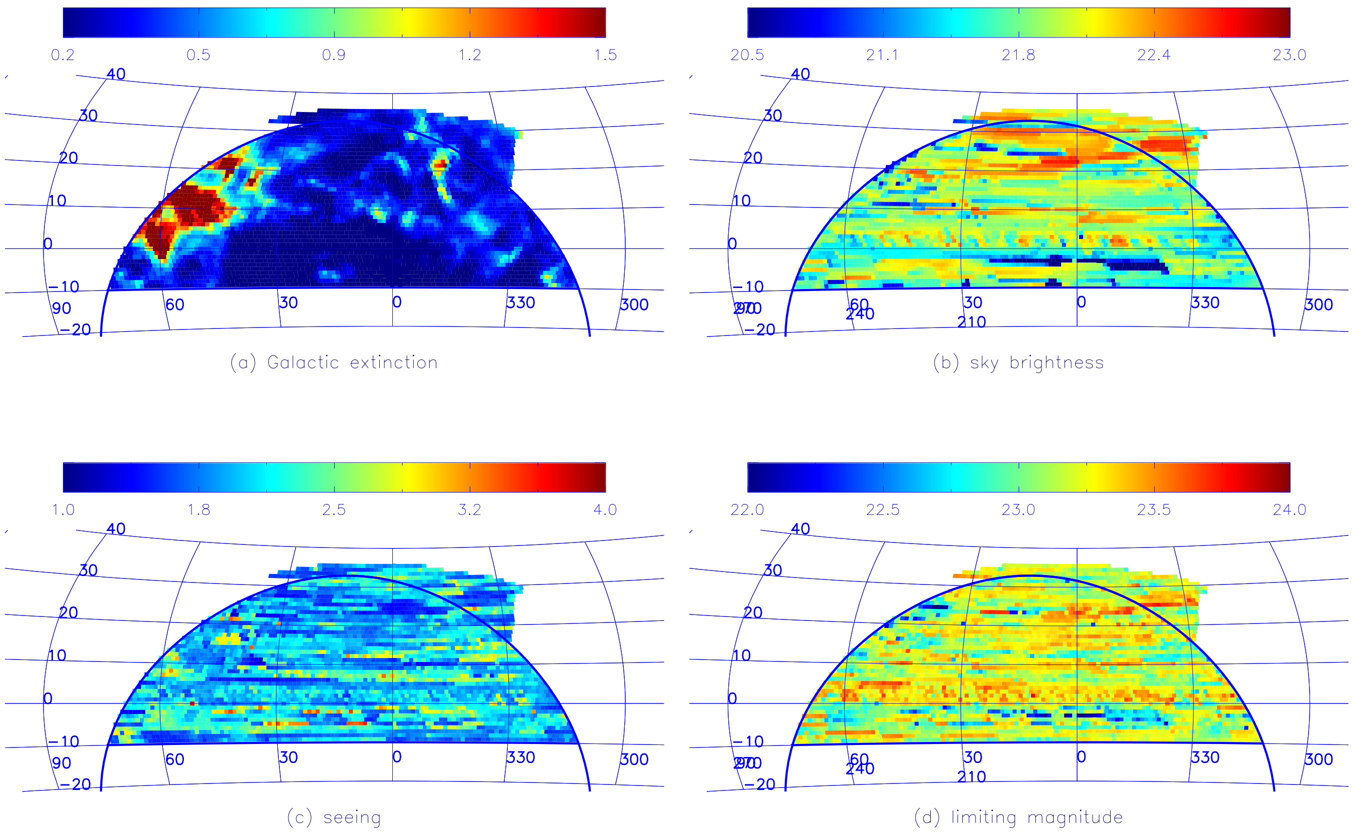

Figure 5. (a): u-band Galactic extinction map in the SCUSS footprint; (b) sky brightness map in mag arcsec^{-2}. (c) Seeing map in arcsec; (d) magnitude limit map in mag.

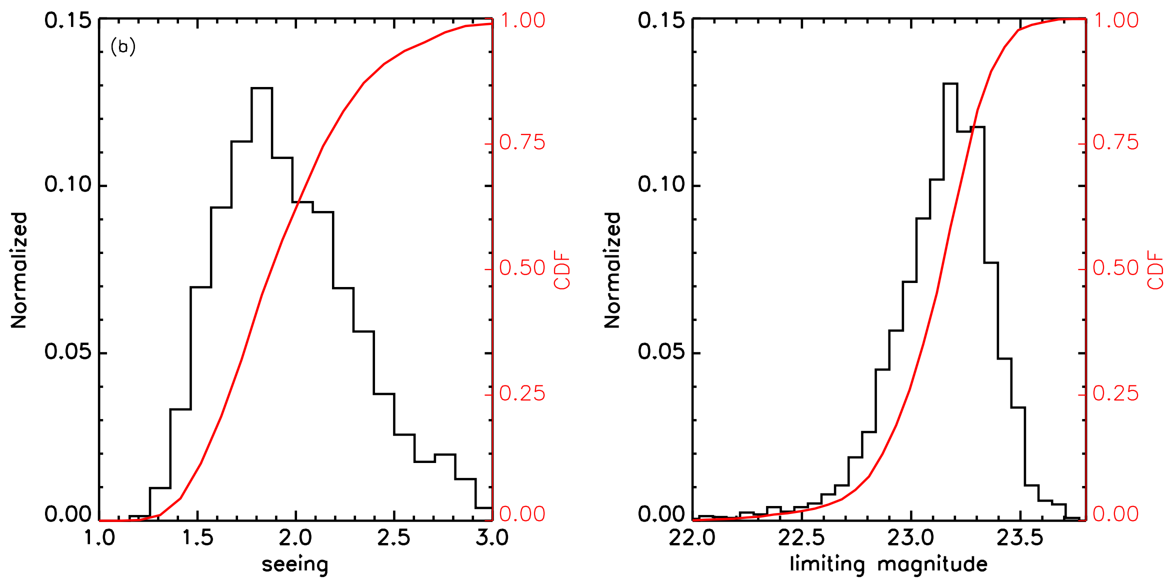

Figure 6. (a): seeing distribution in arcsec (b) magnitude limit distribution. The curves are the cumulative distributions.

PSF magnitudes are converted to the CHFTLS photometric system.[7] The solid and dashed lines in this figure show the photometric rms around the average offset as a function of the magnitude. The SDSS has a much larger offset when the magnitude is fainter. The magnitude offset between the SDSS and the CFHTLS at $u = 23.5$ is about 0.2 mag, while the one between the SCUSS and the CFHTLS is about −0.03 mag. In addition, for the same rms of 0.2, the SCUSS and SDSS magnitude limits are about 22.6 and 21.4 mag, respectively. The SCUSS u band is 1.2 mag deeper.

The overall distributions of the u-band Galactic extinction, sky brightness, seeing, and limiting magnitude are presented in Figure 5. The median u-band Galactic extinction is about 0.096 mag, where the extinction map comes from Schlegel et al. (1998) using the reddening law of Cardelli et al. (1989).

[7] http://cfht.hawaii.edu/Instruments/Imaging/MegaPrime/generalinformation.html

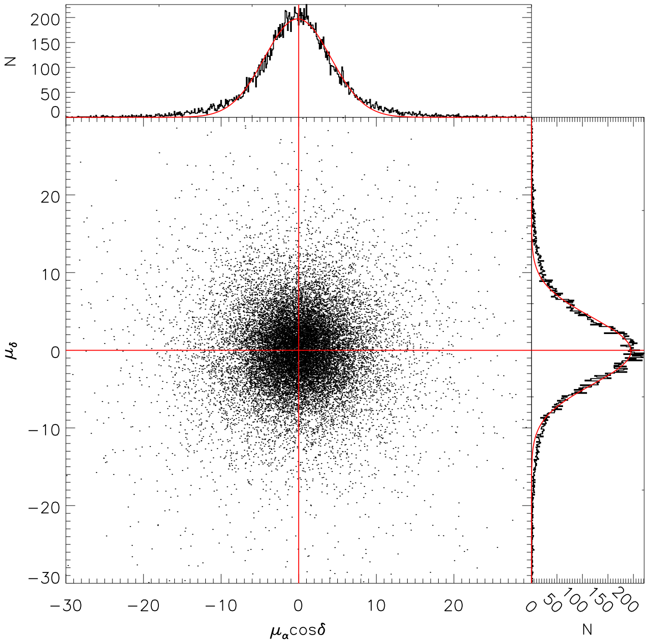

Figure 7. The accuracy distribution of the proper motion derived by the SDSS spectroscopically confirmed quasars. The cross line show the coordinate origin. The red curves in the right and top panels are the Gaussian fits to the distributions of $\mu_\alpha\cos\delta$ and μ_δ, respectively. The units are mas years^{-1}.

Table 4
Columns in the Catalog of Star Proper Motions

Field	Data type	Meaning
ID	LONG	Object ID
RA	FLOAT	R.A. in J2000 (degree)
DEC	FLOAT	Decl. in J2000 (degree)
sigRA	FLOAT	Error of R.A. (mas)
sigDEC	FLOAT	Error of Decl. (mas)
PMRA	FLOAT	Proper motion in R.A. multiplied by cos(δ) (mas years^{-1})
PMDEC	FLOAT	Proper motion in decl. (mas years^{-1})
sigPMRA	FLOAT	Error of proper motion in R.A.
sigPMDEC	FLOAT	Error of proper motion in decl.
MAG	FLOAT	SCUSS automatic magnitude
TYPE	INTEGER	Star/galaxy classification (0 for star; others for galaxy)
OBSNUM	INTEGER	Number of epoches
MeanEpoch	FLOAT	Mean epoch
MinEpoch	FLOAT	Minimum epoch
MaxEpoch	FLOAT	Maximal epoch

Some regions with very high extinctions are not included in the SDSS footprint. Most observations were taken on dark nights, while a few of them were taken at gray time as seen in Figure 5(b). The median seeing is about 2″.0. About 90% of the footprint has seeing better than 2″.5. The *u*-band seeing is usually larger than that in redder bands. The typical *r*-band seeing on Kitt Peak is about 1″.7. The limiting magnitude shown in Figure 5(d) is estimated by using the SExtractor automatic magnitude measurements of 5σ point sources. The median limiting magnitude is about 23.2 mag. About 98.3% of the footprint has a depth fainter than 22.5 mag. The histograms of the seeing and limiting magnitudes and their cumulative distributions are also shown in Figure 6.

5. CATALOG OF STAR PROPER MOTIONS

Peng et al. (2015) used a novel method from Qi et al. (2015) to determine the absolute proper motions of detected objects in SCUSS single-epoch images. Based on data from the SCUSS (2010–2013) and the Guide Star Catalog II (Lasker et al. 2008) (1950–2000), the absolute proper motions of ∼8 million objects were derived. A great deal of effort was put into correcting the position-, magnitude-, and color-dependent systematic errors.

Quasars are distant and regarded to have no proper motion. The accuracy of our proper motions is estimated by using the spectroscopically confirmed quasars identified by the SDSS. Figure 7 displays the distributions of the calculated proper motions of these quasars in R.A. ($\mu_\alpha\cos\delta$) and decl. (μ_δ). The systematic errors (or the average) are about -0.11 and -0.02 mas years^{-1}, and the corresponding random errors (or the standard deviation) are about 4.90 and 4.93 mas years^{-1} for μ_α cos δ and μ_δ, respectively. The Gaussian fitted random errors are 4.27 and 4.35 mas years^{-1}. The random error increases with the magnitude from about 3 mas years^{-1} at $u = 18.0$ mag to about 7 mas years^{-1} at $u = 22.0$ mag. The SCUSS proper motions are compared with those in the SDSS catalog, which shows a high consistency. The typical dispersion of the proper motion between the SCUSS and SDSS is about 5 mas years^{-1}. Table 4 shows the columns in our proper motion catalog.

6. CONCLUSIONS

The SCUSS survey was a collaborative program between the National Astronomical Observatories of China and the Steward Observatory. It used the 2.3 m Bok telescope and wide-field 90Prime camera to survey the northern part of the south Galactic cap in SDSS *u* band. The observations were completed in 2013 and covered about 5000 deg^2. This paper presents the data release of about 4000 deg^2, 92% of which is covered by the SDSS.

We have summarized the survey and data reduction in this paper, and the reader can refer to Zou et al. (2015a) and X. Zhou et al. (2015, in preparation) for more details. The data products include calibrated single-epoch images, stacked images, and photometric catalogs. The catalogs contain the photometry of both SCUSS detected sources and objects in SDSS catalogs and provide magnitude measurements on stacked images and co-added magnitudes from measurements on single-epoch images. The SDSS information are also included in the catalogs with a 2″ matching error. We have analyzed the data quality, such as the sky brightness, seeing, and magnitude limit. The median limiting magnitude (5σ) is about 23.2 mag, which is ∼1.2 mag deeper than the SDSS *u* band. We also release a catalog of star proper motions of about 8 million objects derived by Peng et al. (2015). The data and documentations can be accessed through the SCUSS data release website.[8] In this website, the images and catalogs can be retrieved either by using query forms (developed by the Chinese astronomical data center) or directly through the data directory trees.

This work is supported by the National Natural Science Foundation of China (NSFC, Nos. 11203031, 11433005,

[8] http://batc.bao.ac.cn/Uband/data.html

11073032, 11373035, 11203034, 11303038, 11303043) and by the National Basic Research Program of China (973 Program, Nos. 2014CB845704, 2013CB834902, and 2014CB845702). Z.Y.W. was supported by the Chinese National Natural Science Foundation grant No. 11373033.

The SCUSS is funded by the Main Direction Program of Knowledge Innovation of Chinese Academy of Sciences (No. KJCX2-EW-T06). It is also an international cooperative project between National Astronomical Observatories, Chinese Academy of Sciences, and Steward Observatory, University of Arizona, USA. Technical support and observational assistance from the Bok telescope are provided by Steward Observatory. The project is managed by the National Astronomical Observatory of China and Shanghai Astronomical Observatory. Data resources are supported by Chinese Astronomical Data Center (CAsDC).

SDSS-III is managed by the Astrophysical Research Consortium for the Participating Institutions of the SDSS-III Collaboration including the University of Arizona, the Brazilian Participation Group, Brookhaven National Laboratory, Carnegie Mellon University, University of Florida, the French Participation Group, the German Participation Group, Harvard University, the Instituto de Astrofisica de Canarias, the Michigan State/Notre Dame/JINA Participation Group, Johns Hopkins University, Lawrence Berkeley National Laboratory, Max Planck Institute for Astrophysics, Max Planck Institute for Extraterrestrial Physics, New Mexico State University, New York University, Ohio State University, Pennsylvania State University, University of Portsmouth, Princeton University, the Spanish Participation Group, University of Tokyo, University of Utah, Vanderbilt University, University of Virginia, University of Washington, and Yale University.

Based on observations obtained with MegaPrime/MegaCam, a joint project of CFHT and CEA/IRFU, at the Canada–France–Hawaii Telescope (CFHT) which is operated by the National Research Council (NRC) of Canada, the Institut National des Science de l'Univers of the Centre National de la Recherche Scientifique (CNRS) of France, and the University of Hawaii. This work is based in part on data products produced at Terapix available at the Canadian Astronomy Data Centre as part of the Canada–France–Hawaii Telescope Legacy Survey, a collaborative project of NRC and CNRS.

REFERENCES

Bertin, E., & Arnouts, S. 1996, A&AS, 117, 393
Cardelli, J. A., Clayton, G. C., & Mathis, J. S. 1989, ApJ, 345, 245
Comparat, J., Delubac, T., Jouvel, S., et al. 2015, A&A, submitted (arXiv:1509.05045)
Cui, X.-Q., Zhao, Y.-H., Chu, Y.-Q., et al. 2012, RAA, 12, 1197
Gu, J., Du, C., Jia, Y., et al. 2015, MNRAS, 452, 3092
Jia, Y., Du, C., Wu, Z., et al. 2014, MNRAS, 441, 503
Lasker, B. M., Lattanzi, M. G., McLean, B. J., et al. 2008, AJ, 136, 735
Nie, J. D., Smith, M. C., Belokurov, V., et al. 2015, ApJ, 810, 153
Peng, X., Qi, Z., Wu, Z., et al. 2015, PASP, 127, 250
Qi, Z., Yu, Y., Bucciarelli, B., et al. 2015, AJ, 150, 137
Raichoor, A., Comparat, J., Delubac, T., et al. 2016, A&A, 585, A50
Schlegel, D. J., Finkbeiner, D. P., & Davis, M. 1998, ApJ, 500, 525
York, D. G., Adelman, J., Anderson, J. E., Jr., et al. 2000, AJ, 120, 1579
Zou, H., Jiang, Z.-J., Zhou, X., et al. 2015a, AJ, 150, 104
Zou, H., Wu, X.-B., Zhou, X., et al. 2015b, PASP, 127, 94